Understanding pool-riffle dynamics through continuous morphological simulations

Gustavo Adolfo Mazza de Almeida[1,2] and José F. Rodríguez[1,2]

Received 2 February 2010; revised 21 October 2010; accepted 27 October 2010; published 13 January 2011.

[1] Pool-riffle dynamics is governed by complex time and spatial interactions between water and sediment flows. In the last few decades, significant advances have been made in characterizing and modeling the hydrodynamics of pool-riffle sequences, and this information has been extensively used as the basis of conceptual models to describe or infer pool-riffle morphodynamics. A lot less attention, however, has been paid to the coupled dynamics of flow and sediment, which is essential to fully understand these complex geomorphic systems. This paper uses an unsteady 1-D flow-morphology and bed-sorting model to analyze pool-riffle dynamics. The model is first applied to a pool-riffle sequence on a 1.1 km reach of the lower Bear Creek, Arkansas, United States. After showing the model's ability to describe the general reach hydrodynamics and morphological evolution over 1 year, the detailed sediment and flow information is used to investigate pool-riffle dynamics in terms of self-maintenance mechanisms. Two effects that have been only marginally explored in the past, i.e., bed sediment sorting and downstream riffle control, are explained and quantified with the help of the model's outputs. The results show that self-maintenance occurs more frequently than previously thought as a result of grain sorting and that erosion or deposition of contiguous riffles also constitutes a self-maintenance mechanism. These findings provide the support for a physically based, integral description of pool-riffle morphodynamics and highlight the importance of flow and sediment variability on pool-riffle self-maintenance. The morphodynamic analysis bridges the gap between observations and current theories based mainly on hydrodynamic information.

Citation: de Almeida, G. A. M., and J. F. Rodríguez (2011), Understanding pool-riffle dynamics through continuous morphological simulations, *Water Resour. Res., 47*, W01502, doi:10.1029/2010WR009170.

1. Introduction

[2] An issue that has puzzled geomorphologists for a long time is the ubiquity and persistence of pool-riffle sequences in rivers with different slopes and substrate conditions [*Seddon*, 1900; *Gilbert*, 1914]. More recently, the topic has received increasing attention because of a growing awareness of its crucial importance in establishing habitat diversity in streams [*Rhoads et al.*, 2008]. Human impact on streams has often modified pool-riffle structure either by physically removing them (e.g., through channelization) or by altering pristine flow and sediment conditions in the catchment. Restoration efforts that seek to reestablish natural pool-riffle sequences have revealed the lack of a practical and comprehensive theory of pool-riffle morphodynamics applicable to real-life flow and sediment conditions [*Wade et al.*, 2002; *Rhoads et al.*, 2008].

[3] One of the main complexities of pool-riffle dynamics is that spatial patterns of erosion and aggradation vary with flow conditions. Observations of the mechanisms responsible for the self-maintenance of pools and riffles have shown that during low and medium discharges, aggradation occurs in pools while riffles are eroded. During high-discharge episodes, however, this situation is inverted, and pool erosion takes place while riffles aggrade [*Leopold and Wolman*, 1960; *Andrews*, 1979; *Lisle*, 1979; *Campbell and Sidle*, 1985]. The velocity reversal hypothesis emerged as an attempt to explain this behavior (*Keller* [1971], after *Seddon* [1900] and *Gilbert* [1914]). The hypothesis states that the bottom velocity is less in the pool than in the adjacent riffle at low flows but increases more quickly with discharge until both velocities are equal at discharges close to bankfull flow. Beyond this point, the velocity reversal occurs, and the velocity in the pool is higher than in the riffle. This hypothesis has been extensively used as the basis of many conceptual models of pool-riffle self-maintenance [*MacWilliams et al.*, 2006].

[4] The reversal hypothesis has been investigated in several studies on the basis of the analysis of field [*Keller*, 1971; *Andrews*, 1979; *Lisle*, 1979; *Sear*, 1996; *Bhowmik and Demissie*, 1982; *Hassan and Woodsmith*, 2004; *Thompson and Wohl*, 2009] and laboratory [*Thompson et al.*, 1999; *Rodríguez et al.*, 2004a; *Rhoads et al.*, 2008] data, as well as through hydrodynamic simulations [*Richards*, 1978; *Keller and Florsheim*, 1993; *Carling and Wood*, 1994; *Booker et al.*, 2001; *Cao et al.*, 2003;

[1]School of Engineering, University of Newcastle, Callaghan, New South Wales, Australia
[2]eWaterCRC, Canberra, ACT, Australia

0043-1397/11/2010WR009170

Wilkinson et al., 2004; *Harrison and Keller*, 2007]. Although some studies have shown the occurrence of flow reversal [*Andrews*, 1979; *Lisle,* 1979; *Cao et al.*, 2003; *MacWilliams et al.*, 2006], others have reported that reversal was found only in some of the pools and riffles analyzed or under particular conditions [*Carling and Wood*, 1994; *Sear,* 1996; *Booker et al.*, 2001; *Wilkinson et al.*, 2004] or that reversal did not occur at all [*Richards*, 1978; *Carling*, 1991]. However, most of these researchers agree that convergence in flow variables in the pool and riffle occurs with increasing discharge.

[5] The actual velocity reversal has seldom been recorded because of the difficulty of measuring during bankfull flow. Rather, it has been inferred, deduced, or computed using additional assumptions. Alternative theories of maintenance usually focus on 2- or 3-D flow patterns [*MacWilliams et al.*, 2006; *Thompson et al.*, 1999; *Harrison and Keller*, 2007; *Thompson and Wohl*, 2009; *Booker et al.*, 2001; *Rhoads et al.*, 2008] or on the different characteristics of the bed material or near-bed roughness conditions on pools and riffles [*Clifford*, 1993a; *Sear*, 1996]. The velocity reversal discussion is far from settled, indicating a clear gap in the full understanding of pool-riffle morphodynamics, which requires a rigorous coupling of flow and sediment dynamics including mutual feedbacks.

[6] This paper analyzes pool-riffle morphodynamics using an unsteady 1-D flow morphology and bed-sorting model operated on a continuous basis. Even though 2- or 3-D models are required to fully capture pool-riffle dynamics due to variations in width, secondary flow patterns, and gravitational effects in bed load movement, the 1-D approach used here provides insight into the effects of different sediment sizes in shaping and maintaining the pool-riffle longitudinal profile while limiting computational complexity. The model is first applied to a real-life situation to assess its predictive capabilities in a particular stream reach. Then it is used as a tool to investigate the relevance and the limitations of the velocity reversal hypothesis and to better explain some important mechanisms governing pool-riffle morphodynamics.

2. Self-Maintenance and the Velocity Reversal Hypothesis

[7] From the perspective of basic hydraulics concepts (e.g., 1-D flow mass conservation equation and quasi-steady simplification), higher velocities in pools during the velocity reversal will occur only if the flow area in the riffle is greater than that in the adjacent pool. Considering that riffles generally have higher bottom elevation than pools, riffles should always have shallower flow depths than pools. Therefore, the higher mean velocities in the pool are only possible in situations where the shape of the pool cross section is more contracted than that of the riffle. Several researchers have raised similar concerns [*Caamaño et al.*, 2009; *Cao et al.*, 2003; *Carling*, 1991; *Carling and Wood*, 1994; *Bhowmik and Demissie*, 1982; *Wilkinson et al.*, 2004]. Another rather simplistic argument found in the literature [*Bhowmik and Demissie*, 1982] challenging the reversal hypothesis is that if the highest shear stresses are exerted in the pools during floods, sediment found in the bed surface of pools should be coarser than in riffles, which is contrary to experience [*Bhowmik and Demissie*, 1982; *Reuter et al.,* 2003; *Hirsch and Abrahams*, 1981; *Lisle*, 1979; *Richards*, 1976; *Sear*, 1996; *Rabeni and Jacobson*, 1993; *Leopold and Wolman*, 1957]. The strength of this argument is undermined by *Lisle et al.* [2000], who found that local values of shear stress during bankfull flow and bed grain size were essentially uncorrelated in an analysis of six different reaches in California and Colorado.

[8] The limitations of a reversal hypothesis based on averaged flow variables have driven many researchers to seek an explanation for the observed behavior in 2- and 3-D flow features [e.g., *MacWilliams et al.*, 2006; *Thompson et al.*, 1999; *Harrison and Keller*, 2007; *Thompson and Wohl*, 2009; *Booker et al.*, 2001]. One of the soundest hypotheses is based on the concentration of flow in parts of the channel due to some kind of lateral contraction or obstruction [*MacWilliams et al.*, 2006; *Hassan and Woodsmith*, 2004]. According to this hypothesis, local velocities are considerably stronger in pools than in riffles during high discharges because of the constriction. Also, this effect is "convected" downstream in the form of a jet so that it is not restricted to the constriction itself. This is a meaningful argument for explaining some pool-riffle maintenance, but it requires the presence of a flow contraction or obstruction and does not explain those cases where pools and riffles are found in reaches with relatively uniform width. *Clifford* [1993b, p. 47] argued that "even where a clear relationship exists between obstructions and pool-bar topography, most pools in a riffle-pool sequence do not have obstructions with which they can immediately be associated". Conversely, *Buffington et al.* [2002] observed that flow obstruction was the most significant mechanism responsible for pool formation in forest rivers of northern California, southeastern Alaska, and southern Oregon. Flow concentration can also be associated with convergent areas in alternate bar systems and pools in meandering reaches where the effective flow area can be considerably reduced.

[9] More subtle flow patterns that can be potentially associated with pool-riffle sediment transport are secondary flows. Alternation of flow convergence (in pools) and divergence (in riffles) in straight and meandering reaches due to width and depth variations generates a characteristic secondary circulation pattern that can advect high-momentum fluid toward the bed [*Booker et al.*, 2001; *Rhoads et al.*, 2008]. However, this effect can be stronger during small to medium flows when streamline curvature is more pronounced [*Rodríguez et al.*, 2004b], so its effectiveness as a self-maintenance mechanism is not completely clear.

[10] The review of self-maintenance mechanisms shows that they seem to operate under specific circumstances and that it is difficult to identify a universal process on the basis of flow variables alone. The inclusion of sediment transport processes in the analysis will complement and strengthen a more comprehensive explanation for pool-riffle self-maintenance.

3. Role of Sediment Transport on Pool-Riffle Dynamics

[11] Most of the difficulties in providing reliable predictions of pool-riffle evolution are related to the large number of variables and physical phenomena involved. Although significant progress has been made in understanding

complex properties of flows in pool-riffle sequences, little attention has been devoted to sediment transport itself. To date, only a few published studies have quantitatively determined sediment transport through pool-riffle sequences, and the amount of data is limited [*Campbell and Sidle*, 1985; *Sear*, 1996; *Booker et al.*, 2001; *Hassan and Woodsmith*, 2004]. Conclusions on the maintenance of these morphological features have been based mainly on flow patterns and have neglected more complex sediment transport processes, which are the ultimate drivers of morphology.

[12] Sediment transport seems to be the missing intermediate step between flow and morphology. In particular, fractional transport, longitudinal grain sorting, bed level fluctuations and their feedbacks on flow, and the history of past flows are expected to play a significant role in pool-riffle morphodynamics. If, for instance, a sequence of medium flow episodes is able to produce considerable erosion of the finer fractions in the riffles, pools will have a significant storage of fine material which can be more easily entrained than that of the armored riffles when larger flows occur. This is supported by several observations of deposits of fine sediments in pools [*Gilbert*, 1914; *Andrews*, 1979; *Lisle and Hilton*, 1995]. The deposition of fines in pools by successive medium-flow episodes also reduces their flow area, so that for a given discharge, velocities in the same pools may be significantly different depending on the history of previous episodes. Finally, the hydraulic characteristics (depths and velocities) of a given pool are highly dependent on the control exerted by the riffle immediately downstream [*Richards*, 1978; *Carling*, 1991; *Pasternack et al.*, 2008], and for higher discharges this riffle may also be controlled by the riffle farther downstream. As riffle crest heights can experience significant fluctuations during floods, the idealized hydraulic characterization based on a fixed bed is, at the least, questionable.

[13] One of the main reasons for this gap between flow and morphology is the difficulty in obtaining synchronous detailed information on variables such as fractional sediment transport rates and bed grain size distributions over time, either in the field or the laboratory. Faced with this difficulty, numerical modeling of morphology emerges as an interesting (if not the only) alternative to understand and predict pool-riffle evolution, as it allows the inclusion of different physical mechanisms acting in different time and spatial scales and provides considerably detailed results. A similar approach was used by *Parker et al.* [2008] for studying the dynamics of the armor layer.

4. Model Formulation

[14] The model used here consists of an integration of existing models for flow and sediment dynamics and has conceptual and practical similarities with other 1-D flow-morphological models [*El kadi Abderrezzak and Paquier*, 2009; *Ferguson and Church*, 2009; *Langendoen and Alonso*, 2008; *Papanicolaou et al.*, 2004; *Wu and Vieira*, 2000]. It consists of four components representing the main physical processes discussed in this paper: 1-D unsteady flow, fractional sediment transport, morphodynamics, and grain sorting. The components are solved sequentially at every time step, that is, the flow model produces cross-sectional velocities and depths that are used to compute shear stresses and drive the fractional bed load sediment transport model. Bed load is integrated to determine bed changes, and the transported sediment fractions are used to update the bed composition. The new bed (both in elevation and composition) is then fed back into the flow model to finalize the loop and start a new time step. Details of each of the components are presented in sections 4.1–sections 4.4.

[15] The model is by no means comprehensive, as it incorporates only the set of phenomena deemed strictly necessary to investigate the questions raised in this paper. While this approach limits the model in terms of representativeness in some situations, it allows for focusing on a limited number of processes to obtain meaningful results. Although an effort has been made to represent realistic conditions using field data, the study should still be regarded as a numerical experiment, where important physical phenomena taking place in the real world have been neglected in the model. In particular, the 1-D formulation disregards complex flow features such as flow concentration and secondary currents, which are present even in straight reaches and may have a strong influence on sediment transport and morphology. Other important phenomena not taken into account include bank failure, flow and sediment interaction with vegetation, and changes in soil porosity during bed sorting processes, to name only a few. The results presented in this paper are not an attempt to rigorously test the model, and in the real world these results may be modified by other physical processes. The effects of these other processes on sediment transport (and in particular on pool-riffle self-maintenance) constitute an important avenue for future investigation.

4.1. Hydraulic Model

[16] The hydraulic model solves the Saint-Venant 1-D unsteady flow equations [*Liggett and Cunge*, 1975]:

$$\frac{\partial y}{\partial t} + \frac{1}{B}\frac{\partial Q}{\partial x} = 0, \tag{1}$$

$$\frac{\partial}{\partial t}\left(\frac{Q}{A}\right) + \frac{\partial}{\partial x}\left(\frac{\alpha Q^2}{2A^2}\right) + g\frac{\partial y}{\partial x} + gS_f = 0\,, \tag{2}$$

where t is the time, x is the streamwise coordinate, y is the water surface elevation, B is the flow width, g is the gravitational acceleration, Q is the flow discharge, A is the flow area, α is the nonuniform velocity distribution coefficient, and S_f is the friction slope, obtained using the Manning equation and the conveyance subdivision method [*Brunner*, 2008]. The linearized versions of equations (1) and (2) [*Liggett and Cunge*, 1975] are solved simultaneously by using a generalized form of the *Preissmann* [1961] four-point implicit finite difference scheme. This scheme approximates any variable f, and its derivatives as

$$f(x,t) \approx \theta\left[\psi f_{j+1}^{n+1} + (1-\psi) f_j^{n+1}\right] + (1-\theta)\left[\psi f_{j+1}^{n} + (1-\psi) f_j^{n}\right], \tag{3}$$

$$\frac{\partial}{\partial x} f(x,t) \approx \theta\frac{f_{j+1}^{n+1} - f_j^{n+1}}{\Delta x} + (1-\theta)\frac{f_{j+1}^{n} - f_j^{n}}{\Delta x}\,, \tag{4}$$

$$\frac{\partial}{\partial t} f(x,t) \approx \psi\frac{f_{j+1}^{n+1} - f_{j+1}^{n}}{\Delta t} + (1-\psi)\frac{f_{j}^{n+1} - f_{j}^{n}}{\Delta t}\,, \tag{5}$$

where j and n are space and time indexes, respectively, Δx is the spatial step, Δt is time step, θ is the time weighting factor, and ψ is the space weighting factor. The Preissmann scheme has been extensively tested and used in engineering and science for more than four decades, and its numerical capabilities regarding convergence, stability, and accuracy have been widely documented [*Cunge et al.*, 1980; *Meselhe and Holly*, 1993, 1997; *Kutija*, 1993]. In addition, the model includes procedures to enhance model robustness under near-critical and small-depth conditions, which are known to pose significant challenges to the stability of the solution. For near-critical conditions (Froude numbers between 0.95 and 1) the model linearly reduces a component of the convective momentum term that typically overshoots [*Kutija*, 1993]. Small depths are handled by computing the friction slope using an upstream scheme ($\psi = 1$) when the depth falls below a user-defined value [*Meselhe and Holly*, 1993]. The time step is also automatically reduced in both cases.

4.2. Sediment Transport Model

[17] The *Wilcock and Crowe* [2003] transport model is used in this study for estimating fractional transport rates for mixed sand-gravel sediment. The transport function is defined as

$$W_i^* = \begin{cases} 0.002\phi^{7.5} & \phi < 1.35 \\ 14\left(\dfrac{1-0.894}{\phi^{0.5}}\right)^{4.5} & \phi \geq 1.35, \end{cases} \tag{6}$$

where W_i^* is a parameter representing the rate of transport for size i and ϕ is the relationship between bed shear stress τ and a reference value of shear stress τ_{ri}, i.e.,

$$W_i^* = \frac{(s-1)gq_{si}}{F_i u_*^3} \tag{7}$$

$$\phi = \frac{\tau}{\tau_{ri}} \tag{8}$$

[18] In equations (7) and (8), s is the ratio of sediment to water density, g is the gravity, q_{si} is the volumetric transport rate of size i per unit width, F_i is the fraction of size i in the bed surface, and u_* is the shear velocity. Reference shear stress τ_{ri} may be regarded as the critical shear stress. The value of τ_{ri} for each individual grain size is given by

$$\frac{\tau_{ri}}{\tau_{rsm}} = \left(\frac{D_i}{D_{sm}}\right)^b, \tag{9}$$

where τ_{rsm} is the value of τ_{ri} that corresponds to the mean size of bed surface D_{sm}, and the exponent b is given by

$$b = \begin{cases} 0.12 & \dfrac{D_i}{D_{sm}} < 1 \\ \dfrac{0.67}{1+\exp\left(1.5-\dfrac{D_i}{D_{sm}}\right)} & \dfrac{D_i}{D_{sm}} \geq 1 \end{cases} \tag{10}$$

[19] The reference shear stress for mean grain size depends on the full particle size distribution in the bed and can be modeled as a function of the sand fraction in the mixture:

$$\tau_{rm} = (s-1)\rho g D_{sm}[0.021 + 0.015\exp(-20F_s)], \tag{11}$$

where F_s is the fraction of sand in the surface size distribution.

[20] In 1-D models the use of cross-sectional average shear stress may give rise to significant underestimations of sediment transport rate because of the nonlinearity of bed load relations. In order to improve the estimation of total sediment transport rate, in this work the cross section is subdivided into vertical strips, and the transport formula is applied separately to each strip. The cross-section transport rate of grain size i is the sum of the transport rate in each strip. Shear stress in each strip is estimated using hydrodynamic information as

$$\tau_m = \gamma R_{hm} S_{fm}, \tag{12}$$

where R_{hm} is the hydraulic radius of the individual vertical strip m and S_{fm} is the cross-sectional averaged value of the friction slope that includes only the skin component and is estimated as a function of the sediment diameter using the Manning-Strickler formula.

4.3. Morphological Model

[21] Bed level changes are solved in two steps. First, the 1-D sediment continuity equation (Exner equation)

$$\frac{\partial Q_s}{\partial x} + (1-\lambda)B\frac{\partial z}{\partial t} = 0 \tag{13}$$

is solved, providing the cross-section averaged values of erosion (or sedimentation) ΔZ. In (13) Q_s is the bed load transport, and λ is the porosity of the bed material. The second step consists of distributing ΔZ over the cross section. This is done by weighting local ΔZ values as a function of the transport rate at each point on the bed.

4.4. Grain Sorting Model

[22] The grain sorting model requires knowledge of the bed and bed load grain size distributions, which are continuously changing over time because of erosion, deposition, and alterations in the shear stress spatial distribution. Substrate grain size distribution changes are calculated on the basis of the mass conservation of a thin layer on the bed surface (active layer):

$$(1-\lambda)\left[f_i\frac{\partial z}{\partial t} + \frac{\partial}{\partial t}(F_i L_a)\right] = -\frac{1}{B}\frac{\partial}{\partial x}(Qs_i), \tag{14}$$

where L_a is the active layer thickness, B is the width of the water surface, and F_i is the fraction of sediment size i in the active layer. This equation has the same form as that used by *Hirano* [1971], *Ribberink* [1987], *Parker and Sutherland* [1990], and *Parker* [1991]. The definition of f_i depends on whether erosion or deposition occurs. If erosion takes place, the active layer is displaced downward, incorporating the material of the layer immediately below, and f_i takes the value of the fraction of sediment size i in the layer below. In the case of aggradation, the control volume of the active layer loses particles through the lower boundary as it is displaced upward so that f_i is equal to the fraction of sediment size i in the active layer. The vertical substrate profile is divided into layers that store a particular grain

size distribution. Several layers are necessary to record the history of successive erosion and sedimentation episodes.

5. Model Application

[23] The model has been applied to a reach of Bear Creek, a tributary of the Buffalo River in Arkansas. Field data for this site were acquired by the U.S. Geological Survey as part of a study on habitat dynamics in the Lower Bear Creek [*Reuter et al.*, 2003; *Rabeni and Jacobson*, 1993]. The selected reach (Crane Bottom) is 1100 m long, and its downstream end is situated approximately 1 km from the confluence with the Buffalo River (Figure 1). The reach is entrenched, with a significantly steep bedrock bluff along most of the length of the left bank (see representative cross sections in Figure 2). On the right bank a steep scarp separates the channel from a fluvial terrace that is located approximately 5–7 m above the channel bed. The width of the channel constrained by these steep banks varies between approximately 30 and 40 m. The average slope of the reach is 0.002. Except for the upstream bend, most of the reach is straight, with cross sections of relatively uniform shape, which makes the results of a 1-D model more reliable and also ensures that meandering is not the dominant process in the maintenance of the pool-riffle sequence.

[24] Data available include topography and grain size distribution of the bed in 31 cross sections surveyed four times during the course of the above-mentioned study (June 2001, December 2001, February 2002, and June 2002), as well as nine water surface profiles. The grain size distribution of the material found in the channel varies longitudinally, with reach-averaged values indicating 4.3% in the sand range (0.06–2 mm), 84% gravel (2–64 mm), 10.2% cobble (64–256 mm), and 1.5% boulder (>256 mm). The reach-averaged D_{50} is 29.5 mm. Preliminary runs of the model were conducted using the 31 existing cross sections, but poor model stability at the riffles required the addition of cross sections close to those areas.

[25] Flow data used in the simulation were obtained from a streamflow gauging station in Bear Creek (Figure 3). The data used for most of the year consisted of daily mean discharges, with more detailed time series used during the flood episodes. The first months during the course of the study (June–December 2001) were relatively dry, with the largest daily mean flow of 10.6 m^3/s. For the period between December 2001 and February 2002 two major floods occurred in Bear Creek, with discharges of 310 and 460 m^3/s, respectively. These floods were estimated as approximately 1∼2 and 2∼4 year recurrence intervals, respectively [*Reuter et al.*, 2003]. Between February 2002 and June 2002, four flood episodes with recurrence interval of around 1 year occurred in Bear Creek.

[26] During relatively high flow episodes in the Buffalo River, water surface elevations in Crane Bottom are influenced by backwater effects [*Reuter et al.*, 2003]. To account for this effect, the model was first used to propagate the measured water levels in the Buffalo River up to the downstream part of the study reach. These water levels were then used as the downstream boundary condition of the model. Manning coefficients were estimated from photographs of the site using the *Cowan* [1956] method and personal judgment and then were calibrated using several water surface

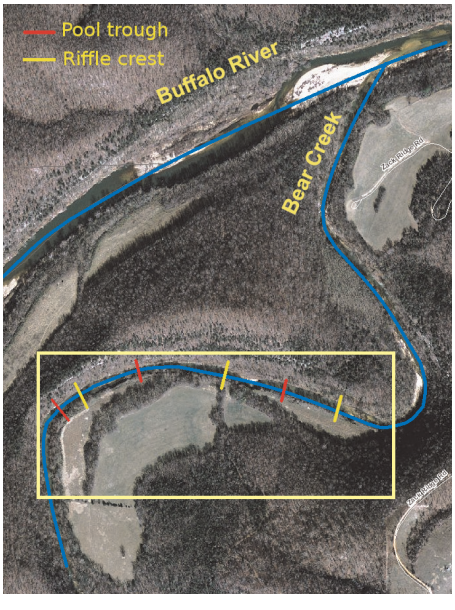

Figure 1. Satellite map showing the Lower Bear Creek and Buffalo River (35°59′37.46″N, 92°41′53.92″W). The rectangle indicates the limits of the study reach. Source for satellite image is the Arkansas Geographic Office.

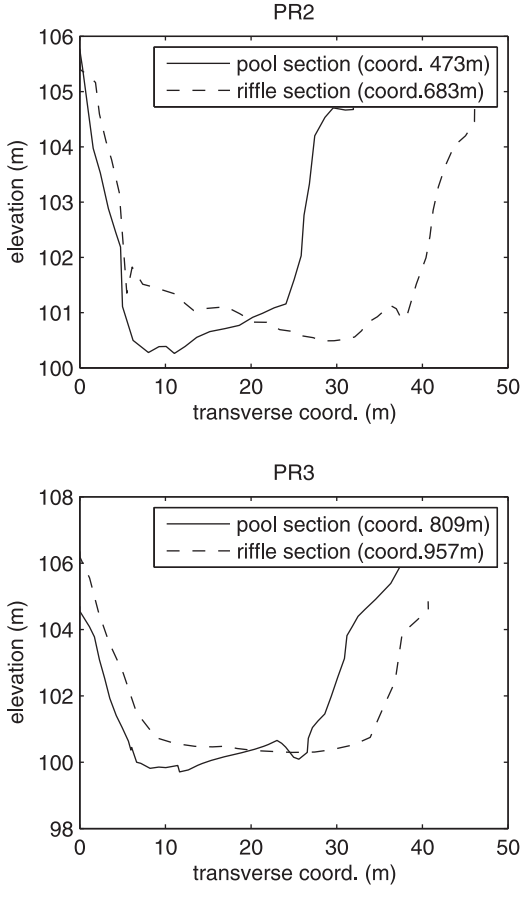

Figure 2. Representative cross sections of pools and riffles (see longitudinal coordinates in Figure 4).

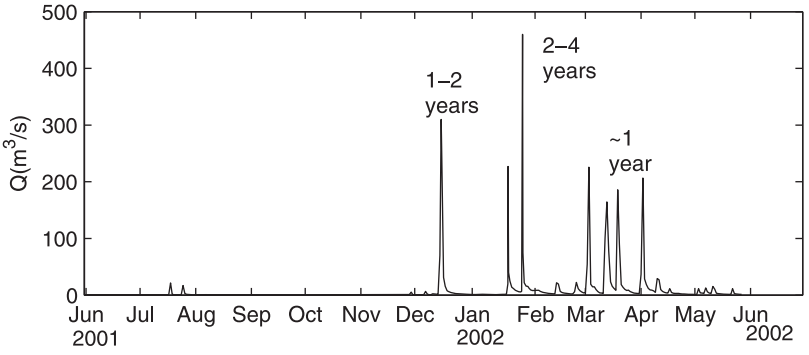

Figure 3. One year flow discharge time series in Bear Creek used in the simulation.

profiles surveyed for different discharges (up to 340 m^3/s) during the course of the *Reuter et al.* [2003] study. Calibrated values had minor differences from the initial estimates.

[27] Reach-averaged sediment transport capacity was used as the upstream boundary condition in the Exner equation (sediment supply to the reach) using a fractional sediment transport–flow discharge relation. This relation was obtained by running a series of steady flow simulations and computing the fractional transport for each one. The size distribution of the sediment inflow was also a function of flow discharge. The choice of reach-averaged transport capacity as the boundary condition is made based on the assumption that the reach is under equilibrium conditions. This assumption is considered reasonable, especially taking into account that alterations driven by changes in sediment supply are associated with longer time scales, in contrast to the few flow pulses used in this simulation. A reach-averaged transport capacity was used to prevent an excessive dependence on a particular cross section (e.g., upstream cross section).

6. Results

6.1. Bed Profile Evolution

[28] Four bed profiles were available for comparison with model outputs: June 2001 (initial), December 2001, February 2002, and June 2002. During the period between June and December 2001 the bed profile of Bear Creek in Crane Bottom experienced no significant changes, which is consistent with the noticeably low discharges in this period (Figure 3). The results of the model at the end of this period perfectly match with measured data of December 2001 and are not shown here for brevity.

[29] In contrast, from December 2001 to February 2002 several flood episodes produced the most significant bed alterations in the course of the year. Figures 4a and 4b compare measured and predicted bed profiles and water surface elevations for February and June 2002, respectively. These are snapshots of the continuous simulation at times when topographical data were available. By observing the water surface profiles in Figures 4a and 4b, one can easily identify three distinct pool-riffle units. The first unit is between sections 0 ($x = 0$) and 350 ($x = 350$) and includes the upstream bend. The deepest part of the bend is at section 218, where the main channel substrate is bedrock. The second and third units are located between sections 350 and 700 and 700 and 1000, respectively. In what follows, these three units will be referred to as PR1, PR2, and PR3, respectively.

[30] Model results in PR1 should be analyzed with care, bearing in mind that secondary currents induced by the bend are not taken into account by the 1-D formulation. It is difficult to determine the extent of the effects of a bend on its downstream reach, but 3-D measurements and numerical simulations of flow in bends [e.g., *Rodríguez et al.*, 2004b] indicate that the helicoidal flow decays rapidly. *Rodríguez et al.* [2004b] reported weak secondary circulation at a sharp bend exit and in the connecting straight reach that followed. Even though these results are strictly valid for low-flow conditions, high-flow conditions do not necessarily result in stronger secondary circulation as the effect of higher velocities is often balanced by smaller streamline curvature.

[31] For the period June 2001 to February 2002 (Figure 4a), results show that the direction of bed alteration (erosion or deposition) has been correctly predicted in 23 out of 31 cross sections. The major differences are in PR1, where the model has predicted a small amount of deposition on the riffle located in section 283, while measured data indicate 20 cm of erosion. Analysis of topographical data for this cross section shows that this erosion occurred only locally (in a 5 m wide portion of the section), indicating the influence of the flow structure induced by the upstream bend. In PR2 (between coordinates 400 and 700) model predictions compare reasonably well with measurements except in the pool (between sections 400 and 500), where predicted erosion is higher than the surveyed data. Finally, in PR3 the model predicted less erosion on the riffle crest compared with surveyed data. Bed changes during the period February–June 2002 were less marked than in the first period, both in the modeled and measured bed profiles. Note that for this period the model predicts a minor erosion of the riffle crest in PR1 (Figure 4b), in contrast to the deposition predicted during the previous period.

[32] Measured and modeled water surface profiles in Figures 4a and 4b compare quite well, and the observed discrepancies are attributable to small differences in height and position of knickpoints in the predicted and surveyed bed profiles. An additional run performed using values of n 20% higher than the calibrated ones revealed only minor differences in the predicted bed profile elevations. This indicated that the morphodynamics model is not overly sensitive to the resistance values and that calibration using water level snapshots is appropriate. Errors in modeled bed

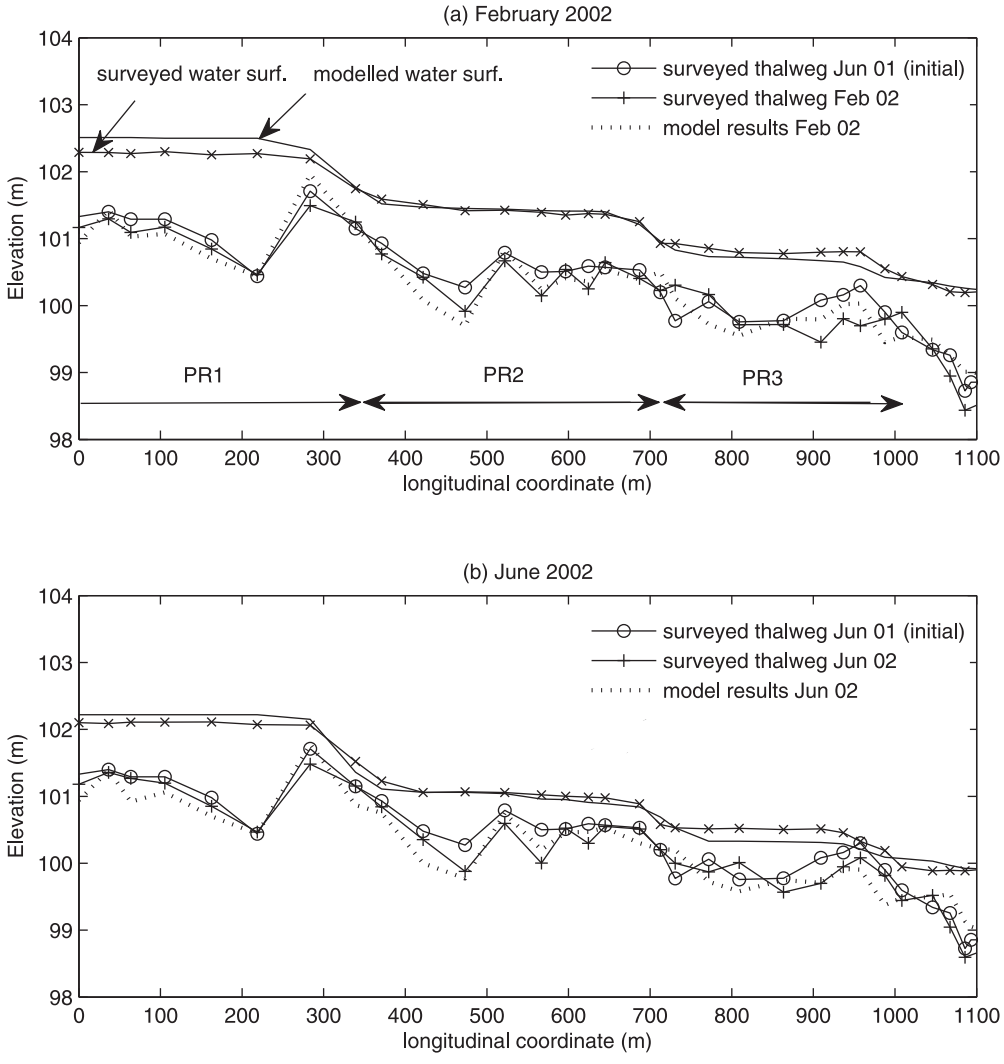

Figure 4. Model results after (a) 8 and (b) 12 months of simulation compared with field data. Water surface and initial bed profiles are also shown. Flow discharges are 5.42 and 1.35 m^3/s, respectively.

profiles may be attributable to several factors, including 2- and 3-D flow features, bank collapse (which is not accounted for in the model), the inherent lack of precision of sediment transport formulae, and the uncertainties associated with spatial variability of bed sediment sizes, to name only a few.

[33] It is important to highlight that the objective of the this comparison is not to suggest that the model can precisely reproduce topographical alterations but to verify that model results reproduce overall spatial patterns of adjustment and that these are of the same order of magnitude as the measured data, so that the model can be used to explore dynamic processes taking place over time. Despite the observed differences, model results show relatively good agreement with measured data. One of the model characteristics of particular interest for the study of pool-riffle dynamics is the ability to capture different bed surface dynamics (erosion or deposition) in pools and riffles as a function of discharge, which is in accordance with field observations. This is illustrated in Figure 5, where pool and riffle transport rates are plotted along with the flow discharge for one particular flood event. Also in Figure 5 is the riffle sediment deficit (i.e., the difference between riffle and pool sediment transport rates), which gives an indication of whether erosion or deposition occurs in the riffle section. Figure 5 shows that during most of the rising limb of the hydrograph the transport rate is lower in the riffle than in the pool, but this trend is reversed during the falling limb. This inversion of transport rates with rising or falling limbs is used here to illustrate the time and spatial dependence of transport and should not be regarded as a rule. The fact that the same discharge produces first sedimentation and then erosion on the riffle highlights one limitation of the velocity reversal hypothesis, as will be discussed in section 6.2.

6.2. Shear Stress Reversal and Sediment Transport Reversal

[34] At this point it is interesting to examine the reversal hypothesis and to investigate its importance in determining sediment transport reversal, which is the ultimate driver for morphological dynamics. Transport reversal is defined here similarly to reversal in flow variables (velocity or shear stress), as the situation when transport in the pool is higher than in the downstream riffle. The relationship between

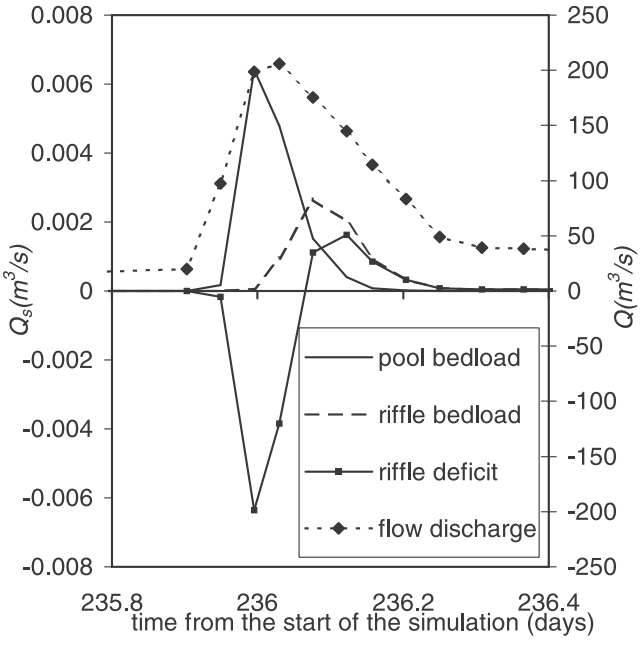

Figure 5. Pool and riffle bed loads and flow discharge time series in PR2.

shear stress and sediment transport reversal has always been assumed as evident in previous studies, as most sediment transport relations are written as a function of bed shear stress. On the contrary, a broader perspective including the role played by longitudinal sorting, selective transport, and stage-dependence of spatial distribution of shear stress on transport reversal is seldom found in the literature (see *Lisle et al.* [2000] for one of the few exceptions).

[35] Figures 6a–6c show the relation between shear stress reversal, represented by τ_p/τ_R, and sediment transport reversal, Qs_p/Qs_R, for the three pool-riffle units. Subscripts p and R indicate pool and riffle sections, respectively. The exact pool/riffle sections used in this comparison are at sections 218/283, 473/683, and 809/957 for PR1, PR2, and PR3, respectively. The choice of riffle sections was based on their role as a control for upstream water elevation, while the deepest section upstream of the riffle was chosen to represent the corresponding pool.

[36] Figure 6 shows that in the Bear Creek simulations the shear stress reversal index τ_p/τ_R reaches maximum values around 1.6 and 1.7 in PR1 and PR2, respectively, and that it is smaller than 1.2 in PR3. This highlights a considerable dependence of reversal on local characteristics. When reversal is expressed in terms of mean velocity (V_p/V_R), the same patterns observed in Figure 6 are reproduced, although the range of V_p/V_R values is relatively smaller than the τ_p/τ_R counterparts (maximum values of approximately 1.2, 1.3, and 1.1 for PR1, PR2, and PR3, respectively).

[37] Figures 6a–6c may be divided into four quadrants, with center coordinates (1,1). If shear stress reversal can be used as a surrogate for transport reversal, data would be concentrated only in quadrants 1 and 3. That is, when pool shear stress is greater than that in the riffle ($\tau_p/\tau_R > 1$), sediment transport in the pool must be greater than that in the riffle ($Qs_p/Qs_R > 1$), and conversely, when $\tau_p/\tau_R < 1$, Qs_p/Qs_R should be also less than unity. However, Figure 6 (especially in Figures 6b and 6c) shows a considerable amount of data in quadrant 2. Quadrant 2 corresponds to a situation where sediment transport is higher in the pool even with higher shear stress in the riffle. This is due to differences in sediment size distributions in pools and riffles. If a certain sequence of low and medium flows is able to relocate fine materials from riffles to pools, the erodibility of pools may be considerably increased, enabling transport reversal before a shear stress reversal takes place. Quadrant 2 events of Figure 6b were situated in the discharge time series in Figure 7. The analysis of Figure 7 shows that these points correspond to the rising limb of most medium and large floods and to the full range of the low-discharge episodes in July 2001.

[38] Transport reversal without shear stress reversal can be explained with the help of Figure 8 for two different situations (July 2001 and January 2002) in PR2. The effect of longitudinal sorting on transport reversal is evident by comparing the bed grain size distribution with fractional transport rates. Transport rates in the pool are markedly higher due to a considerably higher fraction of fine sediment in the pool. In the first case (July 2001), the shear stress reversal index is $\tau_p/\tau_R = 0.30$, and the corresponding transport reversal index $Qs_p/Qs_R = 2.68$, while in January 2002, $\tau_p/\tau_R = 0.59$ and $Qs_p/Qs_R = 1.15$. Model results have shown that bed load transport rates in the pool are sometimes more than 1 order of magnitude higher than riffle bed load transport rates without a shear stress reversal.

[39] Model results indicate that not all floods show the same patterns. If the duration of high-discharge episodes is sufficiently long, more fine sediment is relocated from pools to riffles, reducing the longitudinal grain size disparity between pool and riffle. This redistribution also agrees with some field observations [*Andrews*, 1979]. Figure 9 shows the bed grain size distribution and the corresponding fractional

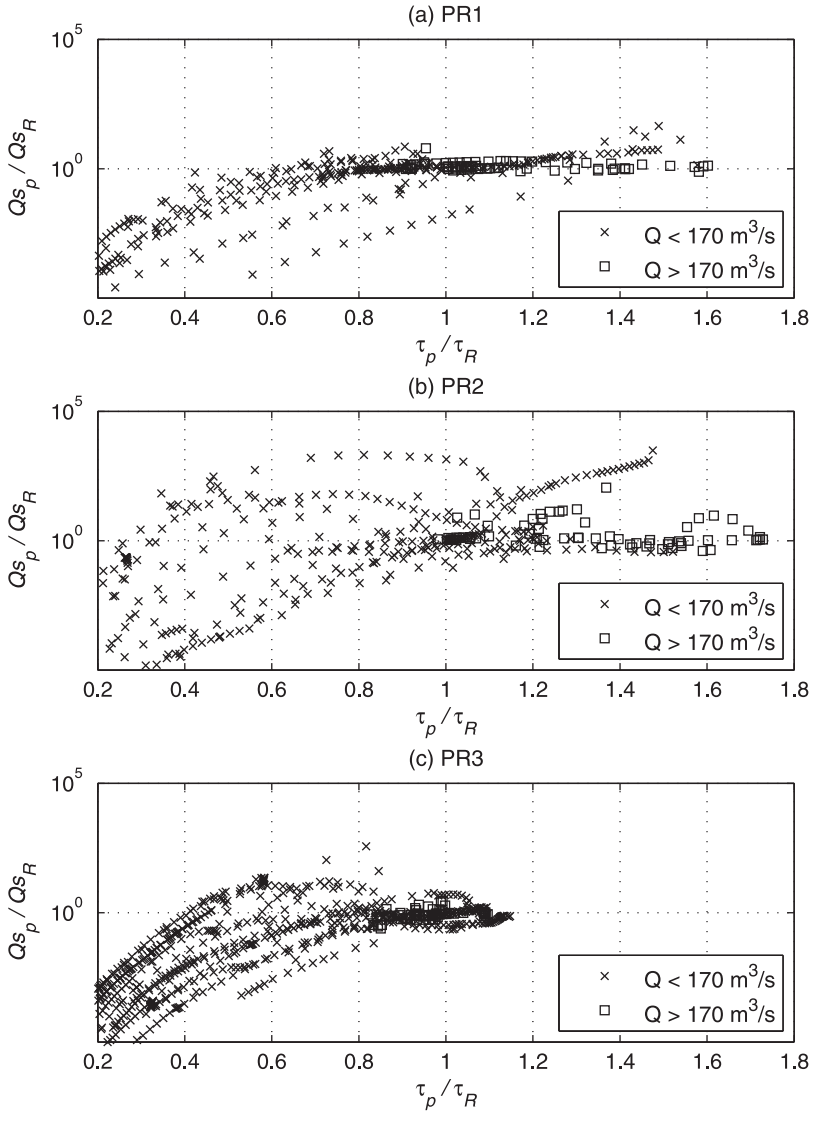

Figure 6. Relation between bed shear stress reversal and sediment transport reversal for three pool-riffle units: (a) PR1, (b) PR2, (c) PR3.

sediment transport before, during, and after the peak discharge of the first flood episode in March 2002. During the very first stages of the flood, the higher fraction of fines in the pool is responsible for a significantly higher transport in the pool ($Qs_p/Qs_R = 45$ and $\tau_p/\tau_R = 0.56$). This significant difference is the result of the higher availability of fines in the pool (which are more easily transported) and the higher mobility of the coarser fractions because of the high percent of

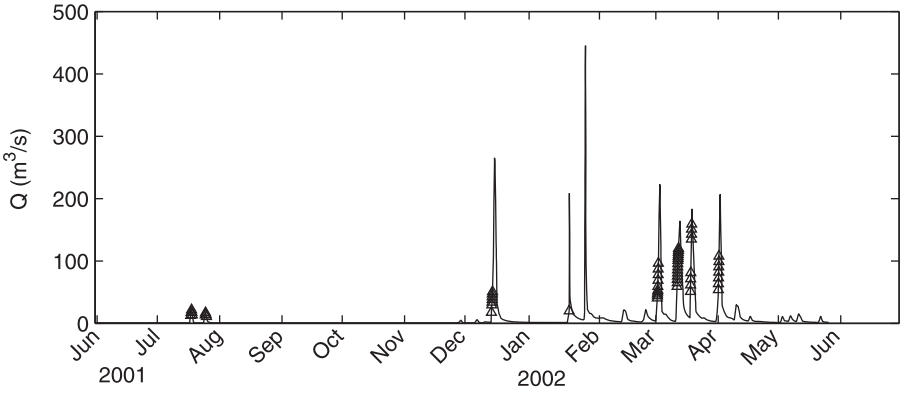

Figure 7. Hydrograph showing points when transport reversal took place without shear stress reversal.

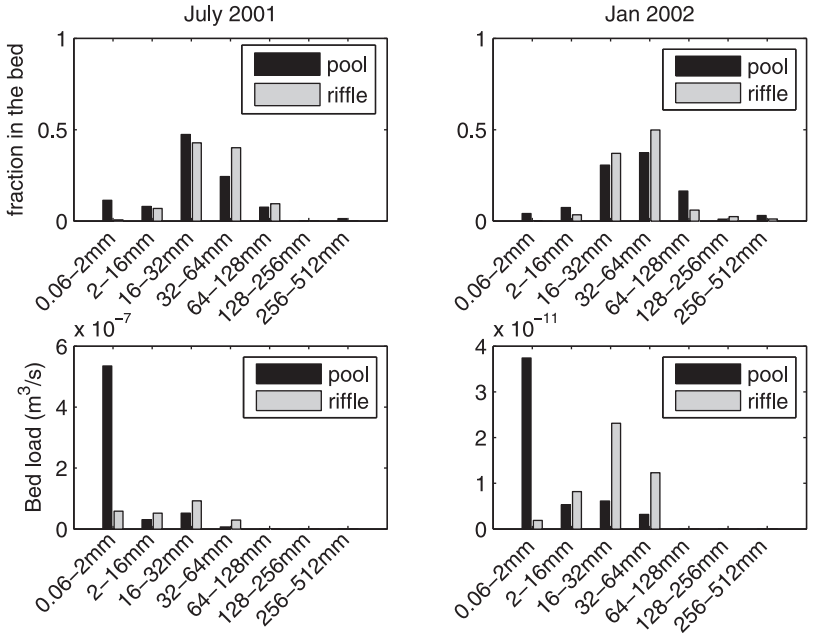

Figure 8. Grain size distribution in the bed and sediment transport by size fraction in two situations (July 2001 and January 2002) when transport reversal took place without velocity reversal. Shear stress reversal index τ_p/τ_R values are 0.30 and 0.59, respectively, while the corresponding Qs_p/Qs_R values are 2.68 and 1.15. Results are in PR2.

sand in the mixture [*Wilcock and Crowe*, 2003]. During the rising limb of the hydrograph this difference in the transport rate of fines produces an equalization of finer fractions and similar bed loads in the pool and in the riffle at the peak discharge ($Qs_p/Qs_R = 1.32$ and $\tau_p/\tau_R = 1.06$). Twenty hours after the peak discharge, when the sand fraction in the pool and in the riffle are of the same order of magnitude, sediment transport is considerably higher in the riffle because of higher

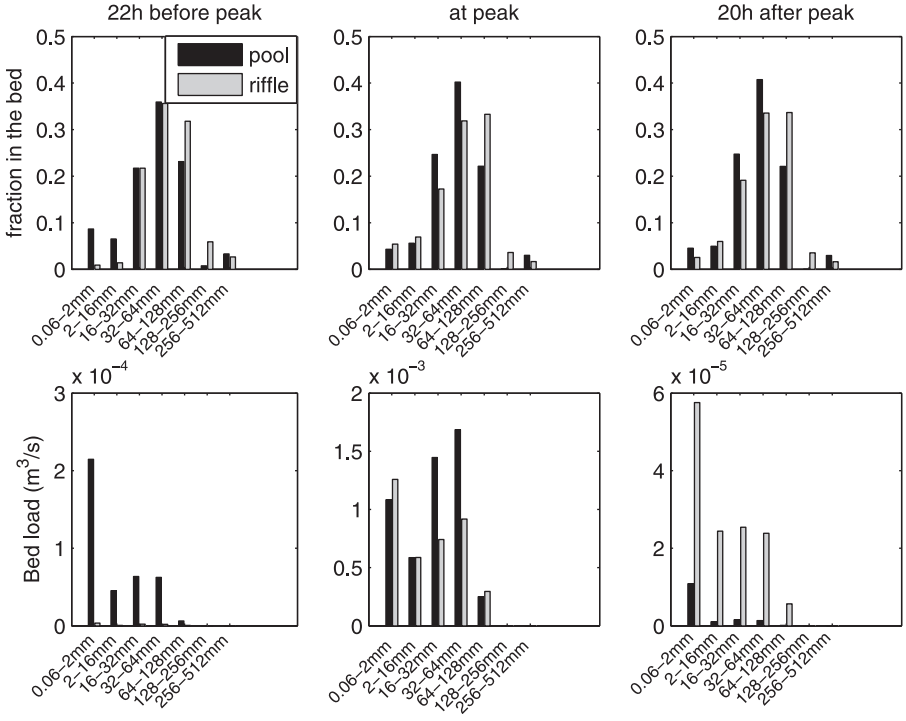

Figure 9. Bed grain size distribution and fractional sediment transport during three different stages of the first flood in March 2002: (left) 22 h before the peak discharge ($Q = 69.0$ m^3/s), (middle) during the peak ($Q = 222.6$ m^3/s), and (right) 20 h after peak ($Q = 68.54$ m^3/s). Results are in PR2.

shear stresses ($Qs_p/Qs_R = 0.10$ and $\tau_p/\tau_R = 0.55$). Comparing the bed load before and after the peak, it is interesting to note that an approximately equal shear stress reversal index produces a considerably different sediment transport in the pool-riffle unit as a function of the size distribution of the bed.

[40] These findings highlight the importance of fractional transport and longitudinal grain sorting on the onset and magnitude of transport reversal. Although the degree of flow reversal is a key variable for pool-riffle morphological dynamics, it should not be regarded as a surrogate of transport reversal. The latter depends on the complex combined effect of different shear stresses and grain size distributions in pools and riffles and on the nonlinear relations governing fractional transport.

[41] It is also worth noting that material coarser than 128 mm was seldom transported (see Figures 8 and 9). The same trend was observed in the field by tracking painted rocks [*Reuter et al.*, 2003].

6.3. Downstream Control and the Interdependence of Pool-Riffle Units

[42] The results presented in section 6.2 have demonstrated that sediment transport reversal should be regarded as a function of the ratio of both shear stress and sediment size between pool and riffle. In particular, it has been shown that, as a result of longitudinal sorting, transport reversal can take place without the need for a shear stress reversal ($\tau_p/\tau_R \leq 1$) due to longitudinal grain sorting. Nonetheless, it must be emphasized that the same results also indicate that flow reversal plays a major role in this functional relation (e.g., only a few data points plot in quadrant 4 in Figure 6). In this section some mechanisms controlling flow reversal are studied independently from sediment transport and grain sorting in order to avoid multiple dependencies and interactions that could obscure the conclusions.

[43] Data in Figure 6 have been divided into two different groups as a function of flow discharge. The division has been carried out to highlight the difficulty in establishing a threshold value for the onset of velocity reversal. The discharge $Q = 170$ m^3/s has been selected in an attempt to estimate a critical value of discharge associated with reversal conditions. In Figures 6a and 6b it is easily recognizable that most of the points for $Q > 170$ m^3/s correspond to shear reversal indexes higher than unity, while most $Q < 170$ m^3/s points correspond to $\tau_p/\tau_R < 1$. The critical value is, however, not indisputable. In Figure 6c, for instance, there is a considerable amount of data for $Q > 170$ m^3/s and $\tau_p/\tau_R < 1$, and in Figures 6a–6c there are a significant number of points with $Q < 170$ m^3/s and $\tau_p/\tau_R > 1$.

[44] Two issues complicate the estimation of a single critical discharge for the onset of shear stress reversal in pools and riffles. First, reversal conditions will seldom be equal in different units because they are highly dependent on differences in cross-section shapes of pools and riffles. So far, no evidence of a general shape-proportion relation supporting the idea of a unique threshold flow for different pool-riffle units has been demonstrated. Second, even for a particular pool-riffle unit, shear stress reversal may take place at different discharges because of downstream control. In the specific case of Bear Creek at Crane Bottom, water surface elevations during floods may be considerably influenced by backwater effects associated with high water levels in the Buffalo River. When the downstream water elevation is sufficiently high, then the riffle may be drowned out, dramatically reducing the differences between pool and riffle water levels. If the downstream-controlled water surface determines an inversion of flow areas between pools and riffles (i.e., riffle cross-sectional flow area becomes greater than the corresponding area in the upstream pool), then flow reversal occurs in an almost discharge-independent fashion.

[45] Even out of the range of influence of tributaries, downstream control is imposed by neighboring riffles, which work analogously to engineering weirs controlling the water surface elevation upstream [e.g., *Richards*, 1978; *Carling*, 1991; *Pasternack et al.*, 2008]. As a result, threshold discharge for shear stress reversal will be dependent on downstream riffle crest elevation (as well as on the shape of downstream riffle section). In order to analyze the influence of downstream riffle elevation on the shear stress reversal index, a series of simulations were carried out in which the elevation of the riffle crest was varied systematically. Steady flow conditions and fixed bed were used to avoid the influence of flow unsteadiness and bed mobility. Backwater effects due to the downstream confluence with the Buffalo River were also eliminated by using a normal-depth (i.e., uniform flow) downstream boundary condition. The influence of riffle crest elevation on the reversal index of the upstream unit was analyzed by increasing the height of the bed in the downstream riffle in PR3 (section 957). This elevation is expected to control water levels downstream of the riffle in PR2, thus determining the threshold discharge for the riffle to be drowned out. Figure 10 presents the relation between discharge and the shear reversal index in PR2 for the initial bed profile along with three bed profiles obtained by increasing the downstream riffle elevation by 20, 40, and 60 cm, respectively. These increments are not unrealistic, as scour chain measurements indicated bed fluctuations greater than 50 cm in 6 out of 18 sections during the period of analysis [*Reuter et al.*, 2003].

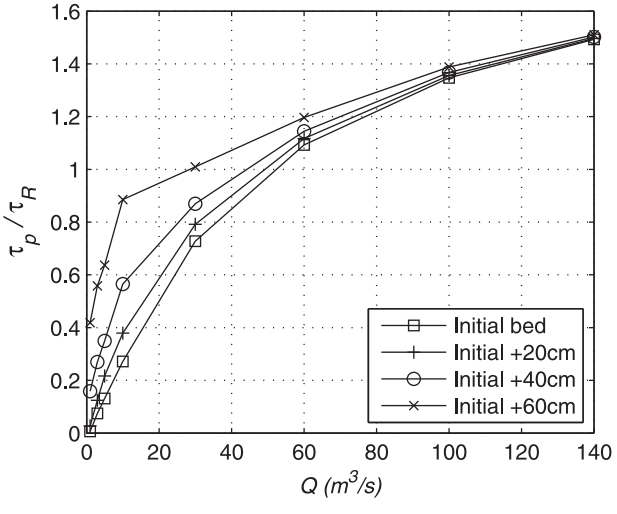

Figure 10. Shear stress reversal index in PR2 as a function of flow discharge. Curves were obtained using the initial bed shape and increasing the elevation of the riffle in PR3 ($x = 957$ m) by 20, 40, and 60 cm.

[46] Figure 10 shows an important mechanism that takes place during floods: changes in riffle elevation due to erosion or deposition affect the dynamics of upstream pool-riffle units. In particular, downstream riffle accretion enhances the conditions for shear reversal to occur in the upstream pool-riffle unit. Riffle erosion effects are more difficult to predict since the control can shift to a nearby section.

[47] Apart from the effect over the upstream unit, riffle crest elevation is also responsible for a second mechanism, which controls the reversal conditions locally in its own unit. The drown-out condition in any given riffle, which directly affects shear stress reversal index and thus influences whether erosion or deposition will occur, is a function of the difference between riffle crest and downstream water elevation. As a result, riffle accretion impairs drown-out conditions and, consequently, the magnitude and frequency of the reversal. Figure 11 is similar to Figure 10, but in this case the elevations were increased at cross section 687 (i.e., riffle of PR2).

[48] The two effects analyzed above often work simultaneously. Figure 12 combines the effect of alteration in the elevation of riffles in PR2 (local) and PR3 (downstream) on the shear stress reversal index in PR2. Each curve in Figure 12 is characterized by the difference between the elevation of riffles in PR2 and PR3 (DZ_{r23}), with $DZ_{r23} = 0.24$ m representing the initial bed elevation. Figure 12 shows that τ_p/τ_R increases with decreasing values of DZ_{r23}.

7. Discussion

[49] The results of the simulations presented in this paper show that both sediment sorting and downstream and local riffle control are effective self-maintenance mechanisms in pool-riffle sequences. Sediment sorting results in selective transport, allowing for the scouring of the pools even in situations in which shear stress is less than in adjacent riffles. The scouring includes the coarser material, as its mobility is enhanced by the presence of fines. Sediment transport adjusts to the material in the bed and can ensure self-maintenance for τ_p/τ_R ratios as low as 0.3 (e.g., Figures 6b and 9). In other words, the inclusion of the grain sorting effect allows for this self-maintenance mechanism to operate more frequently than under the more strict flow reversal requirement. During the 1 year simulation in Bear Creek, for example, shear stress reversal in PR1, PR2, and PR3 occurred during 6, 5, and 4 flow episodes (out of a total of 17 recorded events with peaks greater than 10 m^3/s), while sediment transport reversal occurred 7, 8, and 11 times, respectively. Furthermore, the duration of sediment transport reversal is considerably longer than the corresponding duration of shear stress reversal. Riffles are less likely than pools to have a high proportion of fines because pools preferentially accumulate fines during low flow events; thus, riffles develop armoring and resist erosion by floods.

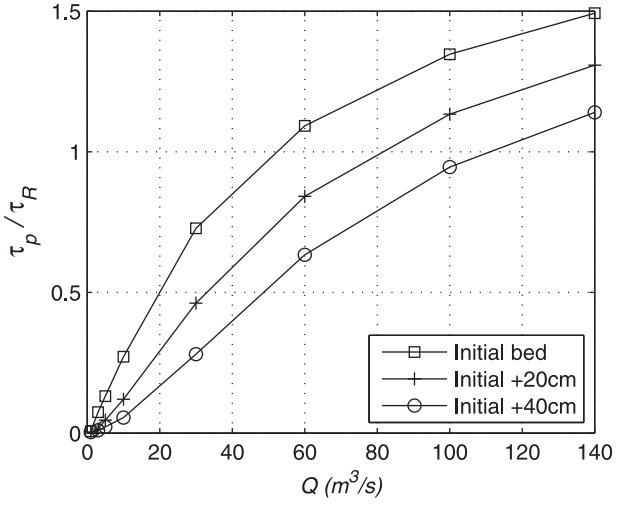

Figure 11. Shear stress reversal index in PR2 as a function of flow discharge. Curves were obtained using the initial bed shape and increasing the elevation of the riffle at PR2 ($x = 687$ m) by 20 and 40 cm.

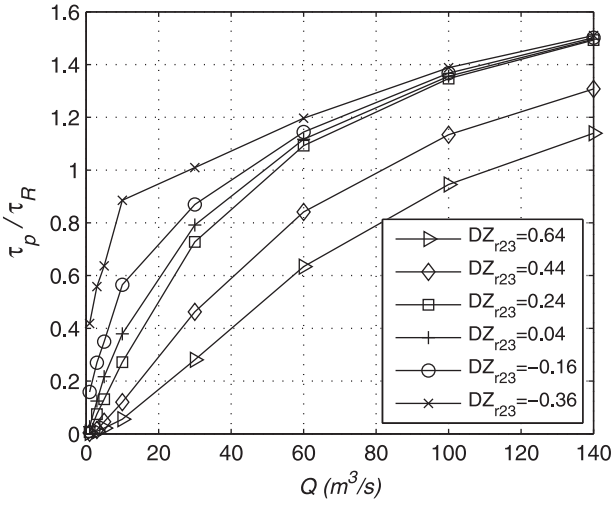

Figure 12. Shear reversal index in PR2 as a function of flow discharge. Curves represent different values of DZ_{r23} (difference between riffle crest elevations in PR2 and PR3).

[50] These findings can be compared with the work of *Parker et al.* [2008], who used the same sediment transport formula and morphological and grain sorting models as the ones used here but used a simpler hydraulic formulation (quasi-steady, uniform flow) and channel shape description (rectangular cross sections and constant initial slope) to study the evolution of bed grain size. *Parker et al.* [2008] report no significant alterations in bed size distribution with time over cycled hydrographs. Substrate composition changes in the Bear Creek simulations can be attributed to varying cross-section shape, irregular longitudinal profile, and the resulting nonuniform flow characteristics. The comparison therefore indicates that spatial nonuniformity of channel form is responsible for time-space grain size alterations in streams. This is a sound hypothesis because grain sorting mechanisms require longitudinal gradients in fractional sediment transport, which can only be achieved through flow nonuniformity. In other words, highly nonuniform flow conditions intimately associated with natural streams are expected to produce alterations in the bed composition under different flows. This is a result of different spatial distribution of shear stresses under different flow discharges, which translates into significant differences in bed load spatial distribution over time. Flow nonuniformity

is an inherent characteristic of pool-riffle sequences, which explains the higher levels of substrate alterations observed over time in these morphological units.

[51] The history of past flow episodes and their effects on sediment availability dictate the likelihood of these self-maintenance events that do not require flow reversal. Sediment transport patterns found in the present study agree with some of the findings of *Campbell and Sidle* [1985], who measured sediment transport in two adjacent riffles in a small Alaskan stream. In particular, those authors found evidence that differences in transport rates in a given riffle during storms were related to the timing, which influenced the amount of fines accumulated in the upstream pool.

[52] Analysis of downstream and local riffle control effects reveals two important mechanisms governing the self-maintenance of pool-riffle sequences. First, the aggradation of a downstream riffle increases the water level and thus the probability and magnitude of flow reversal in the contiguous (upstream) pool-riffle unit (Figure 10). The expected result is enhanced ability of the upstream riffle to aggrade and the pool to erode. Conversely, the erosion of a downstream riffle reduces the probability and magnitude of flow reversal in the upstream pool-riffle sequence, which as a result, becomes more prone to riffle erosion. This mechanism demonstrates the interdependence among different pool-riffle units in a given sequence. Localized alterations on the bed are thus expected to propagate their effects toward neighboring units. Second, the aggradation of a given riffle reduces the probability of flow reversal locally in the same unit (Figure 11), thus increasing the riffle erodibility. On the contrary, an eroded riffle becomes more prone to deposition. This mechanism is an essential self-control that prevents unbounded riffle deposition or erosion.

[53] The combination of both effects, as shown in Figure 12, is an enhancement of shear stress reversal conditions when the difference in the elevation of two contiguous riffle crests is reduced and, conversely, a reduction in τ_p/τ_R when this elevation difference is increased. This elevation-flow feedback mechanism tends to restore or maintain a certain difference in height between riffles, as an increase in the velocity reversal enhances the ability of riffle accretion and vice versa. In other words, when the difference between two contiguous riffle crests is reduced, the upstream riffle becomes more prone to accretion; on the contrary, when this difference is increased, the upstream riffle becomes more prone to erosion. Note that this mechanism always requires the existence of a downstream riffle, so the riffle at the downstream end is the most vulnerable of the sequence. In the absence of any other downstream control, this riffle has only the local control mechanism shown in Figure 11 for self-maintenance, so if a large enough flow erodes it completely, a domino effect may take place propagating upstream and potentially eroding the whole sequence. A similar conclusion has been put forward by *Pasternack et al.* [2008] but without explicitly including the local control mechanism of Figure 11. It must be noted, however, that complete riffle erosion will require substantially larger floods than the ones simulated in this paper, as the results show that material coarser than 128 mm was practically immobile even for a 4 year return period flood.

[54] Both sediment sorting and downstream and local riffle control act simultaneously, reinforcing system self-maintenance. For example, an eroding riffle quickly develops armoring, which reduces erodibility; conversely, an aggrading riffle experiences fining and thus increased mobility, which will favor the downstream and local control feedback. The fact that successive pool-riffle units are so closely linked through these mechanisms may also explain in some cases the spatial organization of the system (pool-riffle spacing) as the strength of these feedbacks are likely to depend on the proximity between units.

[55] As with other pool-riffle maintenance mechanisms, there are situations in which other processes take precedence. For example, *Hassan and Woodsmith* [2004] report no noticeable sorting effect when analyzing three cross-sections in an obstruction formed pool during a flood. However, the results presented in this paper provide indications that sorting does play an important role in the morphology of Bear Creek.

8. Conclusions

[56] The considerable number of variables and interactions influencing pool-riffle morphodynamics indicates that prediction efforts based on simplified assumptions involving solely flow characteristics are seriously limited. In this paper a physically based numerical model integrating unsteady hydraulics, fractional sediment transport, morphological changes, and grain sorting has been used to investigate morphodynamic mechanisms responsible for pool-riffle self-maintenance. A 1.1 km reach of Bear Creek (Arkansas) has been used in the simulations, ensuring realistic topographical, sediment, and flow conditions.

[57] Model results show that longitudinal grain sorting can play a significant role in pool-riffle morphodynamics. In particular, they indicate that sediment transport reversal, which is ultimately responsible for pool-riffle self-maintenance, may occur under flow discharges considerably smaller than those associated with velocity or shear stress reversal. The occurrence of transport reversal without a reversal in the shear stress is a consequence of different grain size distribution in pools and riffles. This finding indicates that pool-riffle self-maintenance mechanisms operate more frequently than had been deduced from the velocity reversal hypothesis. Transport reversal occurred 1.2, 1.6, and 2.8 times more often than shear stress reversal in the three pool riffle units analyzed.

[58] Transport reversal without shear stress reversal occurs under different conditions at each pool-riffle unit because it is highly dependent on the local antecedent grain size distribution at the bed. However, it seems to be more frequent during the rising limb of medium size floods (1∼2 year recurrence). This complicates the definition of a unique critical value of the discharge for all pool-riffle units over which self-maintenance takes place.

[59] Shear stress reversal can occur under different flow conditions at each pool-riffle unit because of local and downstream control exerted by riffles. Riffles erode and aggrade as a result of sediment transport, generating feedbacks on the flow characteristics with consequences for the maintenance of pool-riffle sequences. Two key mechanisms responsible for pool-riffle maintenance have been unveiled. First, the aggradation of a downstream riffle enhances flow reversal probability in the upstream pool-riffle unit via backwater, which induces upstream riffle deposition and

ultimately prevents the formation of a flattened bed. Second, as deposition occurs in a given riffle, the probability of flow reversal in the same pool-riffle unit is reduced, which prevents unbounded riffle deposition. It is the combination of both effects that regulates the difference in height of two contiguous riffle crests.

[60] **Acknowledgments.** This study was supported by eWater CRC. Bear Creek data as well as valuable advice have been provided by R. Jacobson. Comments from B. Rhoads and two anonymous reviewers helped improve the manuscript.

References

Andrews, E. D. (1979), Scour and fill in a stream channel, East Fork River, western Wyoming. *U.S. Geol. Surv. Prof. Pap.*, *1117*, 49 pp.

Bhowmik, N. G., and M. Demissie (1982), Bed material sorting in pools and riffles, *J. Hydraul. Eng.*, *108*, 1227–1231.

Booker, D. J., D. A. Sear, and A. J. Payne (2001), Modelling three-dimensional flow structures and patterns of boundary shear stress in a natural pool-riffle sequence, *Earth Surf. Processes Landforms*, *26*, 553–576.

Brunner, G. W. (2008), HEC-RAS River Analysis System version 4.0, hydraulic reference manual, 411 pp., Hydrol. Eng. Cent., U.S. Army Corps of Eng., Davis, Calif.

Buffington, J. M., T. E. Lisle, R. D. Woodsmith, and S. Hilton (2002), Controls on the size and occurrence of pools in coarse-grained forest rivers, *River Res. Appl.*, *18*, 507–531, doi:10.1002/rra.693.

Caamaño, D., P. Goodwin, J. M. Buffington, J. C. P. Liou, and S. Daley-Laursen (2009), A unifying criterion for the velocity reversal hypothesis in gravel-bed rivers, *J. Hydraul. Eng.*, *135*, 66–70.

Campbell, A. J., and R. C. Sidle (1985), Bedload transport in a pool-riffle sequence of a coastal Alaska stream, *Water Resour. Bull.*, *21*, 579–590, doi:10.1111/j.1752-1688.1985.tb05373.x

Cao, Z., P. A. Carling, and R. Oakey (2003), Flow reversal over a natural pool-riffle sequence: A computational study, *Earth Surf. Processes Landforms*, *28*, 689–705.

Carling, P. A. (1991), An appraisal of the velocity-reversal hypothesis for stable pool-riffle sequences in the river Severn, England, *Earth Surf. Processes Landforms*, *16*, 19–31, doi:10.1002/esp.3290160104.

Carling, P. A. and N. Wood (1994), Simulation of flow over pool-riffle topography: A consideration of the velocity reversal hypothesis, *Earth Surf. Proc. Land.*, *19*(4), 319–332.

Clifford, N. J. (1993a), Differential bed sedimentology and the maintenance of riffle-pool sequences, *Catena*, *20*, 447–468, doi:10.1016/0341-8162(93)90042-N.

Clifford, N. J. (1993b), Formation of riffle-pool sequences: Field evidence for an autogenetic process, *Sediment. Geol.*, *85*, 39–51, doi:10.1016/0037-0738(93)90074-F.

Cowan, W. L. (1956), Estimating hydraulic roughness coefficients, *Agric. Eng.*, *37*, 473–475.

Cunge, J. A., F. M. Holly, and A. Verwey (1980), *Practical Aspects of Computational River Hydraulics*, 420 pp, Pitman, London.

El kadi Abderrezzak, K., and A. Paquier (2009), One-dimensional numerical modeling of sediment transport and bed deformation in open channels, *Water Resour. Res.*, *45*, W05404, doi:10.1029/2008WR007134.

Ferguson, R., and M. Church (2009), A critical perspective on 1-D modeling of river processes: Gravel load and aggradation in lower Fraser River, *Water Resour. Res.*, *45*, W11424, doi:10.1029/2009WR007740.

Gilbert, G. K. (1914), Transportation of debris by running water, *U.S. Geol. Surv. Prof. Pap.*, *86*, 221 pp.

Harrison, L. R., and E. A. Keller (2007), Modelling forced pool-riffle hydraulics in a boulder-bed stream, southern California, *Geomorphology*, *83*, 232–248, doi:10.1016/j.geomorph.2006.02.024.

Hassan, M. A., and R. D. Woodsmith (2004), Bed load transport in an obstruction-formed pool in a forest, gravelbed stream, *Geomorphology*, *58*, 203–221, doi:10.1016/j.geomorph.2003.07.006.

Hirano, M. (1971), River bed degradation with armoring, *Proc. Jpn. Soc. Civ. Eng.*, *195*, 55–65.

Hirsch, P. J., and A. D. Abrahams (1981), Properties of bed sediments in pools and riffles, *J. Sediment. Res.*, *51*, 757–760, doi:10.1306/212F7D9C-2B24-11D7-8648000102C1865D.

Keller, E. A. (1971), Areal sorting of bed-load material: The hypothesis of velocity reversal, *Geol. Soc. Am. Bull.*, *82*, 753–756, doi:10.1130/0016-7606(1971)82[753:ASOBMT]2.0.CO;2.

Keller, E. A., and J. L. Florsheim (1993), Velocity-reversal hypothesis: A model approach, *Earth Surf. Processes Landforms*, *18*, 733–740, doi:10.1002/esp.3290180807.

Kutija, V. (1993), On the numerical modelling of supercritical flow, *J. Hydraul. Res.*, *31*, 841–858.

Langendoen, E. J., and C. V. Alonso (2008) Modeling the evolution of incised streams: I. Model formulation and validation of flow and streambed evolution components, *J. Hydraul. Eng.*, *134*, 749–762, doi:10.1061/(ASCE)0733-9429(2008)134:6(749).

Leopold, L. B., and M. G. Wolman (1957), River channel patterns: Meandering, braided and straight, *U.S. Geol. Surv. Prof. Pap.*, *282-B*, 85 pp.

Leopold, L. B., and M. G. Wolman (1960). River meanders, *Geol. Soc. Am. Bull.*, *71*, 769–794, doi:10.1130/0016-7606(1960)71[769:RM]2.0.CO;2.

Liggett, J. A., and J. A. Cunge (1975), Numerical methods of solution of the unsteady flow equations, in *Unsteady Flow in Open Channels*, edited by K. Mahmood and V. Yevjevich, pp. 89–179, Water Resour. Publ., Fort Collins, Colo.

Lisle, T. (1979), A sorting mechanism for a riffle-pool sequence, *Geol. Soc. Am. Bull.*, *90*, 1142–1157.

Lisle, T. and S. Hilton (1999), Fine bed material in pools of natural gravel bed channels. *Water Resour. Res.*, *35*, 1291–1304.

Lisle, T. E., J. M. Nelson, J. Pitlick, M. A. Madej, and B. L. Barkett (2000), Variability of bed mobility in natural, gravel-bed channels and adjustments to sediment load at local and reach scales, *Water Resour. Res.*, *36*, 3743–3755, doi:10.1029/2000WR900238.

MacWilliams, M. L. Jr., J. M. Wheaton, G. B. Pasternack, R. L. Street, and P. K. Kitanidis (2006), Flow convergence routing hypothesis for pool-riffle maintenance in alluvial rivers, *Water Resour. Res.*, *42*, W10427, doi:10.1029/2005WR004391.

Meselhe, E. A., and F. M. Holly Jr. (1993), Simulation of unsteady flow in irrigation canals with dry bed, *J. Hydraul. Eng.*, *119*, 1021–1039.

Meselhe, E. A., and F. M. Holly Jr. (1997), Invalidity of the Preissmann scheme for transcritical flow, *J. Hydraul. Eng.*, *123*, 652–655.

Papanicolaou, A. N., A. Bdour, and E. Wicklein (2004), One-dimensional hydrodynamic/sediment transport model applicable to steep mountain stream, *J. Hydraul. Res.*, *42*, 357–375.

Parker, G. (1991), Selective sorting and abrasion of river gravel. I: Theory, *J. Hydraul. Eng.*, *117*, 131–149.

Parker, G., and A. J. Sutherland (1990), Fluvial armour, *J. Hydraul. Res.*, *28*, 529–544.

Parker, G., M. Hassan, and P. Wilcock (2008) Adjustment of the bed surface size distribution of gravel-bed rivers in response to cycled hydrographs, in *Gravel-Bed Rivers VI: From Process Understanding to River Restoration*, edited by H. Habersack, et al., pp. 241–285, Elsevier, Amsterdam.

Pasternack, G. B., M. K. Bounrisavong, and K. K. Parikh (2008), Backwater control on riffle-pool hydraulics, fish habitat quality, and sediment transport regime in gravel-bed rivers, *J. Hydrol.*, *357*, 125–139, doi:10.1016/j.jhydrol.2008.05.014.

Preissmann, A. (1961), Propagation des intumescences dans les canaux et rivières, paper presented at 1st Congress of the French Association for Computation, Grenoble, France.

Rabeni, C. F., and R. B. Jacobson (1993), The importance of fluvial hydraulics to fish-habitat restoration in low-gradient alluvial streams, *Freshwater Biol.*, *29*, 211–220, doi:10.1111/j.1365-2427.1993.tb00758.x.

Reuter, J. M., R. B. Jacobson, and C. M. Elliott (2003), Physical stream habitat dynamics in lower Bear Creek, northern Arkansas, *Biol. Sci. Rep. 2003-0002*, 122 pp., U.S. Geol. Surv., Columbia, Mo.

Rhoads, B. L., M. H. Garcia, J. Rodríguez, F. Bombardelli, J. Abad, and M. Daniels (2008), Methods for evaluating the geomorphological performance of naturalized rivers: Examples from the Chicago metropolitan area, in *Uncertainty in River Restoration*, edited by D. Sears and S. Darby, pp. 209–228, John Wiley, Chichester, U. K.

Ribberink, J. (1987), Mathematical modeling of one-dimensional morphological changes in rivers with non-uniform sediment, Ph.D. dissertation, Delft Univ. of Technol., Delft, Netherlands.

Richards, K. S. (1976), The morphology of riffle-pool sequences, *Earth Surf. Processes*, *1*, 71–88, doi:10.1002/esp.3290010108.

Richards, K. S. (1978), Simulation of flow geometry in a riffle-pool stream, *Earth Surf. Processes*, *3*, 345–354, doi:10.1002/esp.3290030403.

Rodríguez, J. F., F. M. López, C. M. García, and M. H. García (2004a), Laboratory experiments on pool-riffle sequences designed to restore channelized low-gradient streams, in *Protection and Restoration of Urban and Rural Streams*, edited by M. Clar et al., pp. 339–348, Am. Soc. of Civ. Eng., Reston, Va.

Rodríguez, J. F., F. A. Bombardelli, M. H. García, K. Frothingham, B. L. Rhoads, and J. Abad (2004b), High-resolution numerical simulation of flow through a highly sinuous river reach, *Water Resour. Manage.*, *18*, 177–199, doi:10.1023/B:WARM.0000043137.52125.a0.

Sear, D. A. (1996), Sediment transport processes in pool-riffle sequences, *Earth Surf. Proc. Land.*, *21*, 241–262.

Seddon, J. A. (1900), River hydraulics, *Trans. Am. Soc. Civ. Eng.*, *43*, 179–229.

Thompson, D. M., and E. E. Wohl (2009), The linkage between velocity patterns and sediment entrainment in a forced-pool unit, *Earth Surf. Processes Landforms*, *34*, 177–192, doi:10.1002/esp.1698.

Thompson, D. M., E. E. Wohl, and R. D. Jarrett (1999), Velocity reversals and sediment sorting in pools and riffles controlled by channel constrictions, *Geomorphology*, *27*, 229–241.

Wade, R. J., B. L. Rhoads, J. Rodríguez, M. Daniels, D. Wilson, E. E. Herricks, F. Bombardelli, M. Garcia, and J. Schwartz (2002), Integrating science and technology to support stream naturalization near Chicago, Illinois, *J. Am. Water Resour. Assoc.*, *38*, 931–944.

Wilcock, P. R., and J. C. Crowe (2003), Surface-based transport model for mixed-size sediment, *J. Hydraul. Eng.*, *129*, 120–128, doi:10.1061/(ASCE)0733-9429(2003)129:2(120).

Wilkinson, S. N., R. J. Keller, and I. Rutherfurd (2004), Phase-shifts in shear stress as an explanation for the maintenance of pool-riffle sequences, *Earth Surf. Processes Landforms*, *29*, 737–753, doi:10.1002/esp.1066.

Wu, W., and D. A. Vieira (2000), One-dimensional channel network model CCHE1D 2.0—Technical manual, *Tech. Rep. NCCHE-TR-2000-1*, Natl. Cent. for Comput. Hydrosci. and Eng., Univ. of Miss., University.

G. A. M. de Almeida and J. F. Rodríguez, School of Engineering, University of Newcastle, University Drive, Callaghan, Newcastle, NSW 2308, Australia. (gustavo.dealmeida@newcastle.edu.au)